





Spatiotemporal dynamics of fine dead surface fuel moisture content in a Colorado mixed-conifer forest

Gunnar C. Ohlson^{A,*}, Chad M. Hoffman^A, Wade T. Tinkham^B, L. Scott Baggett^B and J. Kevin Hiers^C

For full list of author affiliations and declarations see end of paper

*Correspondence to:

Gunnar C. Ohlson Department of Forest and Rangeland Stewardship, Colorado State University, Fort Collins, CO, USA Email: Ohlson@colostate.edu

Received: 12 April 2025 Accepted: 25 October 2025 Published: 19 November 2025

Cite this: Ohlson GC et al. (2025) Spatiotemporal dynamics of fine dead surface fuel moisture content in a Colorado mixed-conifer forest. International Journal of Wildland Fire 34, WF25086. doi:10.1071/WF25086

© 2025 The Author(s) (or their employer(s)). Published by CSIRO Publishing on behalf of IAWF.

This is an open access article distributed under the Creative Commons Attribution-NonCommercial 4.0 International License (CC BY-NC)

OPEN ACCESS

ABSTRACT

Background. Dead fine fuel moisture content (FMC) is critical for predicting fire behavior and effects. Spatiotemporal variation in FMC occurs due to to variability in atmospheric conditions at the fuel interface, which is influenced by interacting factors including local forest structure and topography. Previous research has primarily examined these patterns over coarse spatial scales and relied on few factors to explain variability. Aims. In this study, we monitored the spatiotemporal variability in FMC and characterized how controls of FMC vary over a fire season. FMC was sampled at 80 locations 21 times (approximately weekly) through the summer season in a 17.6 ha southern Rocky Mountain mixed-conifer forest. Key results. Results indicate that FMC variability declines during drier periods and that the influence of forest structure and topography on FMC is constant through time under fluctuating precipitation patterns. FMC values are autocorrelated over spatial and temporal scales and are highly variable over fine spatial scales. Conclusions. Understanding the full magnitude of FMC variability is important for achieving management objectives under both prescribed and wildfire conditions. Implications. Further research into FMC variability and its controls could lead to more reliable models and tools allowing managers to better predict fire behavior and effects.

Keywords: Colorado, forest structure, FMC, fuel moisture, heterogeneity, kriging, microclimate, mixed-conifer forest, moisture dynamics, prescribed fire, spatial variability, spatiotemporal variogram, wildfire, wildland fuels,

Introduction

The moisture content of wildland fuels is critical in the prediction of fire ignition probability (Jurdao et al. 2012) and behavior (Rothermel 1972; Burrows 1999; Fernandes et al. 2008). In addition to being a key factor in fire danger rating indices worldwide (McArthur 1967; Bradshaw et al. 1984; Wagner 1987) and a critical input for many fire behavior models (Bradshaw and McCormick 2000; Linn et al. 2002), fuel moisture content is also essential for developing prescribed fire plans (Ryan et al. 2013; Nyman et al. 2015).

Downed dead fuels are categorized into four size classes based on their 'time lag', or how quickly they adsorb and desorb moisture, which approximately correspond to their diameter (Fosberg et al. 1970). The 1-h fuels have diameters less than 0.6 cm and are the predominant fuel component contributing to ignition success, fire sustainability, rate of spread and intensity in ecosystems characterized by frequent, low-severity surface fires (Loudermilk et al. 2012). The loading, distribution and moisture content of dead, fine fuels are thought to drive spatial and temporal variability in fire behavior and effects (Turner and Romme 1994; Knapp and Keeley 2006). Previous research has shown there is considerable spatiotemporal variability in fine dead fuel moisture content (FMC) (Hiers et al. 2019; Kane 2021), though its accurate characterization in heterogeneous forest structures and topographies over varying climatic conditions has remained elusive. For the purposes of this study, FMC refers to the moisture content of fine dead fuels.

Spatial and temporal variability in FMC is controlled both directly and indirectly through interactions among a suite of biotic and abiotic factors (Tanskanen et al. 2006; Holden and Jolly 2011; Cawson et al. 2024). The influence of these controls depends largely on the spatial scale of investigation, resulting in a hierarchical organization of environmental processes (Ellis et al. 2022; Little et al. 2024). At a global scale, there is increasing evidence supporting an FMC drying trend driven by climate change (Liu 2017). Ellis et al. (2022) report that over the past 41 years, 35.9% of biomes globally have experienced an increase in fire season days with FMC levels below 10%, which the authors considered a critical threshold needed to support extreme fire behavior. In contrast, their study identified only 3.8% of biomes showing a trend toward increasing fuel moisture. At continental scales, latitude, elevation and climate oscillations (such as the El Niño-Southern Oscillation) influence climate and fuel type, thereby shaping patterns of FMC at broad scales (Veblen et al. 2000). For example, studies have linked El Niño-induced drought during spring and summer in the Colorado Front Range to the widespread desiccation of dead fuels and subsequent increased fire occurrence (Schoennagel et al. 2005; Sherriff and Veblen 2008).

At regional to local scales, environmental controls such as vegetation structure and topographic aspect exert substantial influence over FMC dynamics (Nyman et al. 2015; Kane 2021; Little et al. 2024). Nyman et al. (2015) found large variation in FMC at relatively fine scales (10s-10,000s of metres) due to aspect-related differences in solar exposure. Kane (2021) observed that untreated, more densely vegetated stands in northern California, USA, showed an increase in average FMC compared with treated, lower-density stands. Many studies that have examined the moderating effects of forest structure and aspect on FMC have found a pronounced effect from both understory and canopy vegetation structure - where denser vegetation results in wetter dead fine surface fuels (Biddulph and Kellman 1998; Tanskanen et al. 2006; Kane 2021). These results are not surprising given decreased insolation and ventilation levels in denser stands (Moon et al. 2013; Cannon et al. 2019). However, other studies have found a limited effect of vegetation structure on FMC (Faiella and Bailey 2007; Estes et al. 2012; Pickering et al. 2021). For example, Faiella and Bailey (2007) found that mean FMC varied over intraseasonal temporal scales, across study sites, but not across treatment types (control, burn only, thin and burn) in an Arizona ponderosa pine (Pinus ponderosa Lawson and C. Lawson)dominated forest. One potential explanation for this disagreement among previous studies is the climate in which they were conducted - where wetter or more humid climates may create a greater effect of vegetation structure on FMC. Although there are comparatively few studies quantifying the effect of aspect on dead fine FMC, one study in the Ozark Mountains of Missouri found that topographical aspect had the greatest effect on FMC during moderately wet conditions and little effect on FMC during very dry or very wet conditions, suggesting that solar exposure may play an important regulatory role apart from extremes (Stambaugh et al. 2007).

This inconsistency among studies suggests an interaction between vegetation structure and aspect with climate wetness at the local to regional scale.

Previous studies and methodologies have largely been developed to provide coarser-scale estimates of both FMC and its controls while overlooking potential variations at finer scales (Hood et al. 2017; Kane 2021). FMC processes as well as the environmental controls that mediate it operate at finer scales than they are typically measured or evaluated at (Kreve et al. 2018). For example, in these studies, the forest stand often serves as the experimental unit and several FMC observations within each stand are oftentimes collected from large areas in a haphazard manner, in effect averaging out finer, within-stand spatial variations of FMC (e.g. Faiella and Bailey 2007; Kane 2021). Mean data at the forest stand level are also commonly used to estimate the various controls of moisture content, often by averaging metrics like basal area or tree density by treatment unit or type (e.g. Faiella and Bailey 2007; Kane 2021).

At the within-stand scale, FMC is thought to fluctuate in response to temperature, solar radiation and humidity conditions at the fuel interface (Viney 1991; Kreye et al. 2018; Little et al. 2024). Local variability in aspect and vegetation structure further buffer within-stand microclimates from local to regional-scale climate (Nyman et al. 2015; Kreye et al. 2018; Pickering et al. 2021). Tree and understory canopies scatter and absorb solar radiation, altering irradiance into the forest floor. Heterogeneous forest structures consisting of individuals, clumps and openings, common in restored ponderosa pine forests (Churchill et al. 2013), likely share similar processes, albeit down-scaled, to coarser, stand-scale FMC dynamics. Tree canopy openings with lower vegetation density allow greater irradiance and wind ventilation, facilitating lower FMC and quicker moisture desorption (Moon et al. 2013; Hardwick et al. 2015; Kane 2021). Likewise, clumps with greater vegetation density allow decreased irradiance and ventilation, facilitating greater FMC. Pickering et al. (2021) observed this effect in Australian wet eucalypt forests, where understory vegetation helped maintain cooler and wetter conditions below the canopy. Additionally, denser vegetation reduces precipitation throughfall to surface fuels, compared with open forest structures (Crockford and Richardson 2000; Thomas 2016). As a result, in more open areas, we would expect greater FMC fluctuations because of greater precipitation throughfall during precipitation events and quicker moisture desorption during dry periods because of irradiance and wind ventilation. These observations indicate that the fine-scale heterogeneity within forest structure could mirror, in a down-scaled manner, the broader FMC dynamics observed at the stand scale, shaping variability in moisture adsorption and desorption within a single stand.

As few studies have analyzed fine-scale patterns of fuel moisture, information on the influence of vegetation structure and aspect across temporal scales through varying precipitation patterns remains a need in many regions to predict fire behavior and fire effects outside of extreme conditions. The central Rocky Mountains are characterized by an annual pronounced bimodal precipitation distribution with peaks in spring and mid-summer (Kuo and Cox 1975), which are expected to play a pivotal role in shaping FMC dynamics. Early and late summer dry periods contrast with convective rainstorms during the mid-summer North American monsoon (Kuo and Cox 1975; PRISM Climate Group 2020). By monitoring how these precipitation patterns interact with the biotic and abiotic controls of FMC, our study aims to characterize FMC at within-stand scales, contributing to a more comprehensive understanding of wildfire risk in this region.

The objective of this study was to characterize the spatial and temporal resolution of seasonal patterns of FMC spatial variability and the controls that influence that variability within a forest stand over one fire season. Specifically, we asked: (1) is within-stand FMC spatial variability consistent over temporal scales under varying precipitation conditions? (2) Are FMC values spatially autocorrelated at within-stand scales (2–450 m), and do they exhibit consistent semivariance across observation days and intraseasonal periods? (3) Are the environmental controls (understory cover, canopy cover, heat load index) of FMC consistent in

their influence over temporal scales and under differing precipitation conditions? The results of this study provide clarification on the fine-scale spatial variability of FMC and the temporal dynamics of its controls. These findings will help refine modeling tools and assist managers in more accurately predicting fire behavior and effects, particularly during marginal prescribed fire conditions.

Methods

Study site

We conducted this study on the 17.6 ha Pikes Peak Forest Dynamics Plot (400×440 m) in the Pike San Isabel National Forest, Colorado, USA (39.010° , -105.005° , Fig. 1). This site was established in 2016 through a collaboration between Colorado State University, the USDA Forest Service Rocky Mountain Research Station and Region 2 of the USDA Forest Service to monitor long-term forest dynamics following a restoration treatment. The site has a dry continental climate with most precipitation arriving through springtime (March–May) snow events and summertime (July–August) monsoonal storms. The 30-year average precipitation of the site is 638 mm, with average yearly

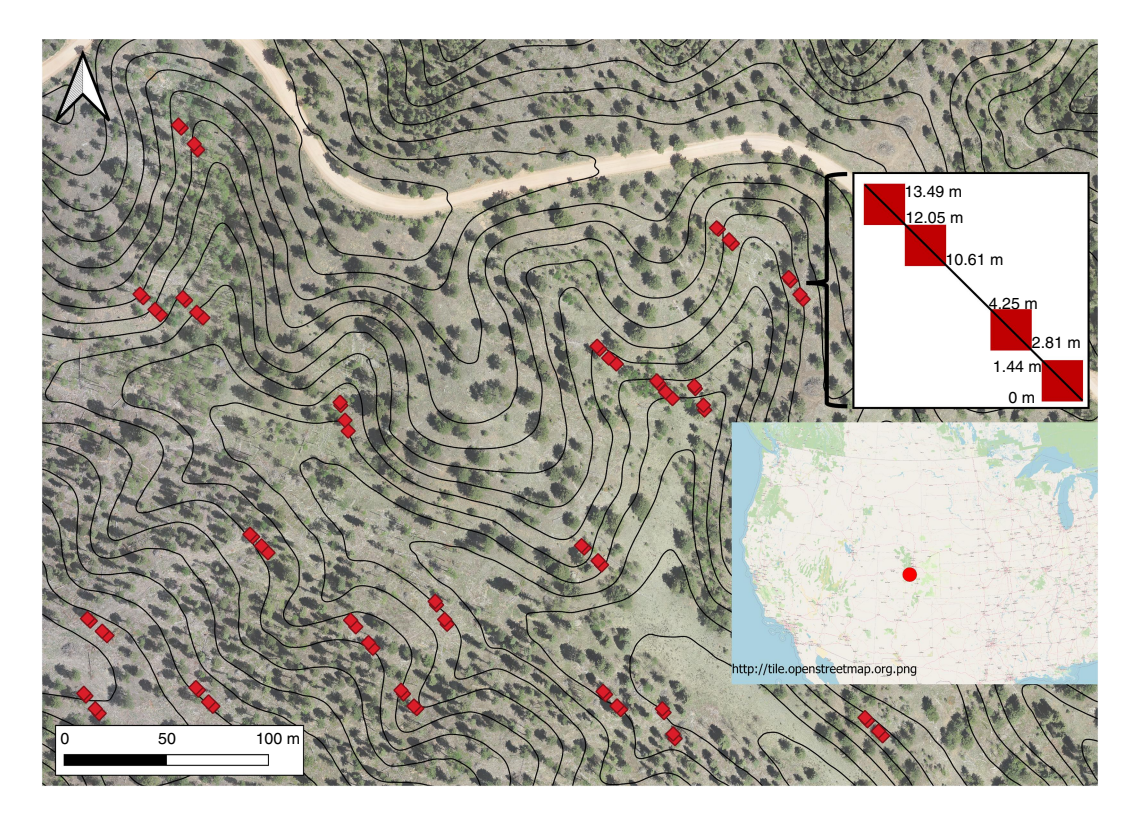


Fig. 1. Map of the Pikes Peak Forest Dynamics Plot in the Pike San Isabel National Forest, approximately 8 km east of Woodland Park, Colorado. Imagery derived from uncrewed aerial system and US Geological Survey (USGS) 3D Elevation Program (United States Geological Survey 2021) derived contour lines (2.5 m interval). Red squares indicate plot locations (n = 80). The top inset diagram shows a within-grid cell, four-plot cluster with plots arranged diagonally and the bottom shows the site location within the United States.

minimum, maximum and average temperatures of -2.5, 11.8, and 4.7°C, respectively (PRISM Climate Group 2020). During the observation period, May to October 2022, the site received 346 mm of precipitation, with average minimum, maximum and average temperatures of 6.4, 20.3 and 13.2°C, respectively. Precipitation levels were 86% of the 30-year average (PRISM Climate Group 2020). Based on data from the Rampart Range Remote Automatic Weather Station (RAWS, NWS ID 053605), during the entire observation period, 70 of the total 150 (46.6%) days received a measurable amount of precipitation. These rain events were concentrated in July and August, with drier periods in June and September. Just in the month of July, the site received a measurable amount of precipitation on 26 of the 31 (83.8%) days.

The site consists of Sphinx gravelly and coarse sandy loam well-drained soils (granitic parent material) on steeper slopes, with more organic matter in valley bottoms and swales. The study site ranges in elevation from 2795 to 2830 m, with plot slopes varying from 2° to 22°. The aspects are predominantly northeast or south-facing. The site is composed of two dominant forest communities dictated by slope and aspect. The more mesic, north-facing slopes are dominated by Engelman spruce (Picea engelmannii Parry ex Engelm.) and Douglas-fir (Pseudotsuga menziesii Mirb.) whereas the more xeric south-facing slopes are dominated by ponderosa pine with intermixed groves of quaking aspen (Populus tremuloides Michx.) in valley bottoms and drainages. The historical fire return interval is estimated to be between 61 and 70 years (LANDFIRE 2020). In 2019, the site underwent a variable retention restoration treatment consistent with regional forest management objectives related to fire hazard reduction and tree spatial arrangement. The mean residual basal area is 12.8 m² ha⁻¹, ranging from 2.6 to 23.9 m² ha⁻¹ depending on aspect and species dominance, with greater densities retained on northerly aspects but with local variation due to openings and tree clumps (see Appendix 1: site overstory and understory summary statistics). Understory vegetation is dominated by sedges, low-stature forbs, common juniper and graminoids (Appendix 1).

Data collection

All trees greater than 1.37 m tall in the site were spatially mapped and diameter at breast height (DBH), species and crown base height were recorded before and after the treatment. The site was divided into 440 20 $\,\times$ 20 m grid cells using measuring tapes. Validation of tree locations using an Emlid Reach RS3 sub-meter GPS (Global Positioning System) unit showed a mean error less than 0.1 m.

We utilized a clustered sampling design to achieve a range of spatial lag distances between sampling locations. Using a stratified selection approach, we chose 20 grid cells for subsampling. To capture the full range of forest and topographical conditions, we chose eight grid cells in ponderosa pine, eight in Engelman spruce and Douglas-fir dominated forest and four in aspen-dominated forest. This stratification ensured that samples best captured the variation in forest structure, aspect and hillslope location, covariates important for explaining sub-canopy solar radiation and precipitation interception. Additionally, grid cells within 20 m of a road or site boundary, containing large machine slash piles, or showing significant mechanical soil disturbance were excluded from the selection process.

Within each of the 20 grid cells, a cluster of four 1.2 \times 1.2 m plots was established along a diagonal line from the southeast to the northwest corner at consistent distance intervals (0-1.7, 2.8-4.5, 10.6-12.3 and 12.3-14 m, Fig. 1), resulting in lag distances between observation locations from 1.7 to 460 m. The plots were monumented using stake whiskers placed in the ground at each distance interval. Each plot was further divided into 36 20 \times 20 cm subplots. On each observation day, the same subplot within each plot (n = 80 plots) was randomly chosen for destructive sampling. We sampled 22 times, approximately weekly from mid-May to mid-October starting at 11:00 am and finishing at approximately 12:30 pm. The second observation day (26 May 2022) was excluded from the analysis owing to residual snow on the ground from a late-season storm occurring between observation days, and observations from one plot were omitted owing to its inexplicable, highly unusual wet condition. This resulted in a total sample size of 1659 observations owing to the omission of 101 observations.

We collected the entire Oi horizon (woody debris less than 0.6 cm in diameter, tree and shrub canopy leaf litter, and detached herbaceous litter) from the randomly chosen subplot within each plot on each observation day (Fig. 2b). Conifer cones, animal waste, bark flakes and ground fuels were omitted from the samples. The samples were placed in labeled and pre-weighed polyethylene resealable bags (Fig. 2c) and transported to the Woodland Park Public Library for immediate weighing on an analytical balance with a precision of 0.01 g. After weighing, the fuels were transferred to paper bags and transported to the Colorado State University Wildland Fire and Fuels Lab in Fort Collins, Colorado, where they were oven-dried at 105°C until no further weight loss was observed, following methods introduced by Matthews (2010). We then calculated gravimetric fuel moisture content (Eqn 1, mass of water per oven-dried mass). The sample wet weight was determined by subtracting the polyethylene bag weight from the total sample mass, and the sample dry weight was calculated by subtracting 20.716 g, the average weight of 50 oven-dried paper bags, from the oven-dried sample mass.

Fuel moisture content = $\frac{\text{(sample wet weight - sample dry weight)}}{\text{(sample dry weight)}} \times 100 \text{ (1)}$

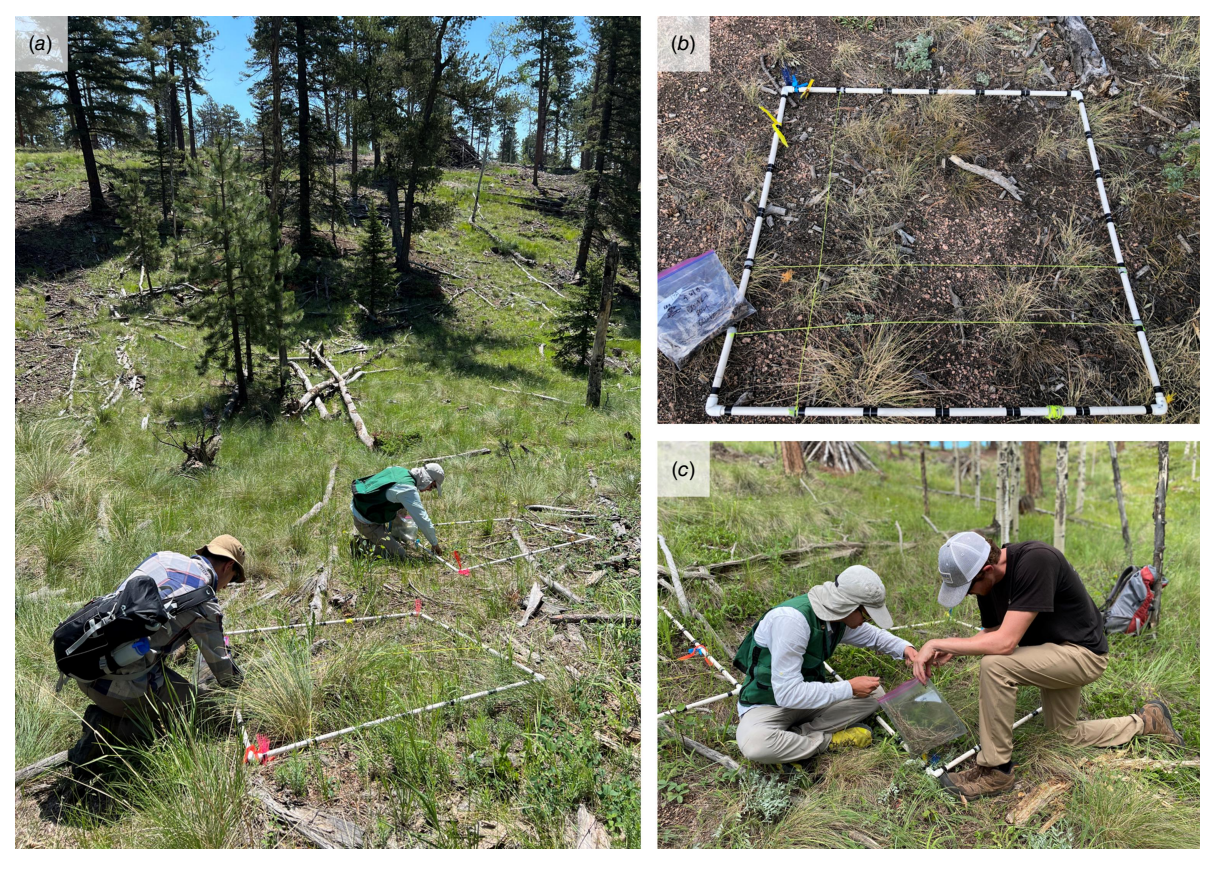


Fig. 2. (a) Post-treatment forest structure and two people sampling fuels from the 0 to 1.7 m and 2.8 to 4.5 m plots within the clustered design. (b) A plot placed between two whiskers to mark the distance intervals and the strings stretched across the PVC sampling frame to denote the randomly generated 20 × 20 cm subplot for collecting the plot's observation. Black markings on the PVC sampling frame are at 20 cm intervals to create the grid of 36 subplots. (c) Two people collecting a dead fine fuel sample into a pre-labeled and pre-weighed polyethylene resealable bag.

Tree crown diameters were calculated for each tree using site and species-specific allometric equations developed from a stratified sample for each species across the range of tree sizes (see Appendix 2). Percentage canopy cover was calculated using the open-source Geographic Information System application QGIS and the sf package in R (Pebesma and Bivand 2005, 2023; R Core Team 2024). Buffers with radii of 2, 4, 6, 8 and 10 m around each plot were created in QGIS. The st_intersection function in the sf package was then used to calculate the area of overlap between the plot buffers and tree canopy cover. Although nadir-based estimates of tree canopy cover may not capture the full effect of tree shading on understory fuels, we used them because they could be calculated across the entire study area (necessary for regression kriging) and aligned with our research focus, investigating the effect of canopy cover over differing precipitation patterns. Percentage understory cover was ocularly estimated at each plot using the average of two observer estimates of herbaceous and live woody fuels. We calculated the McCune and Keon (2002) heat load index with aspect folded around the north-south line (folded aspect = 180 - |aspect - 180|) using a 1 m resolution elevation model from the USGS 3D Elevation Program (United States Geological Survey 2021). This unitless index includes folded aspect, slope and latitude as input variables.

We calculated a site-level precipitation metric by summing antecedent rainfall over 5, 11, 35 h, and 3-, 6-, 9-, 12-, 15-, 18- and 21-day time windows preceding each FMC sampling period and evaluated the Pearson correlation coefficient for each pairing of FMC and precipitation window, like the approach of Crawford et al. (2025). Precipitation data were obtained from the nearest RAWS, which, although not co-located, represents the closest available data source given the absence of on-site rainfall measurements. Though rainfall conditions may differ slightly between the RAWS and the study site owing to their 5 km separation, the RAWS is located within the same forest type and at a similar elevation, so any discrepancies are likely minor. Although both precipitation event duration and amount have been found to be relevant weather events impacting the moisture content of dead fuels (Diószegi et al. 2023), we calculated cumulative precipitation amount rather than duration owing to the high-intensity, yet short-duration nature of afternoon monsoonal rainstorms characteristic of the site and season of our observation period.

Analysis

FMC spatial variability

We organized the data into three intraseasonal periods to assess spatial autocorrelation and variability over time. These three periods have distinct trends in precipitation amount and frequency both historically and during the period of study, with a dry early summer period, a wet monsoonal period occurring in mid-summer and a drier late summer period (PRISM Climate Group 2020). We calculated the mean, median and standard deviation of FMC observations of each period; then, we constructed boxplots for each observation day to investigate FMC spatial variation over temporal scales. We constructed cumulative distribution function plots of each intraseasonal period to evaluate the likelihood of different FMC levels occurring and calculated the proportion of observations above and below a 30% moisture of extinction threshold for forest floor fuels (Rothermel et al. 1986). Lastly, we constructed kernel density plots for each intraseasonal period and calculated skewness and kurtosis values to assess distribution shape of the three periods.

To assess and model FMC variations over spatial and temporal scales, we used a spatiotemporal variogram and kriging approach. Using the gstat package in R, we computed an empirical spatiotemporal variogram using a spatial cutoff distance of 15 m and temporal lags ranging from 0 to 5 days. (Pebesma 2004; Gräler et al. 2016; R Core Team 2024). Model parameters were then extracted for evaluation, like the approach of Snepvangers et al. (2003). The best-performing variogram model was the sum-metric semivariance model consisting of wave covariance functions for the spatial, temporal and spatiotemporal processes, following the approach of O'Rourke and Kelly (2015). In datasets where observations vary in both spatial and temporal dimensions, the variogram is a useful tool in identifying and characterizing space-time dependence by interpolating values at unvisited locations and times (Snepvangers et al. 2003). Using the fitted sum-metric variogram model, we then performed universal spatiotemporal kriging for the 15th day of each observation month (15 May 2022, 15 June 2022, 15 July 2022, 15 August 2022, 15 September 2022, 15 October 2022) using the krigeST function in the gstat package (Pebesma 2004; Gräler et al. 2016). We chose a universal kriging approach because it has been shown to outperform other spatial interpolation methods when modeling fuel attributes at this site (Hoffman et al. 2023). The kriging model included log-transformed FMC as the response variable with heat load index as the covariate. We selected heat load index and canopy cover as covariates because these metrics are available at both plot and site scales, improved model performance (see Appendix 3) and influence FMC (Nyman et al. 2015; Kane 2021).

Environmental control effect on FMC

We used a generalized additive model (GAM) in the mgcv package (Wood 2017) specified with a gamma distribution and natural log link function to assess the effect of vegetation structure and heat load on FMC and if the effects of those controls depended on current precipitation (Hastie 2017). GAMs are a useful semi-parametric model because they allow for non-linear relationships between continuous predictors and the response by utilizing flexible smoothing functions (Pedersen et al. 2019). To assess vegetation structure effect on FMC and allow for simple non-linear relationships, we used smoothed understory cover and canopy cover terms, and we used a smoothed heat load index term to assess the effect of topography on FMC. We used tensor product smooths with the three interaction terms to assess the varying effect of canopy cover, understory cover and heat load index on FMC through differing precipitation levels.

The choice of variables to measure and include in our analysis was motivated by firmly established and previously researched ecological interactions and mechanisms like the approach of Bradford *et al.* (2017). To assess multicollinearity among variables, we constructed a correlation plot with all variables and FMC. All buffer scales of canopy cover were collinear at the >0.65 level and the 2 m scale had the greatest correlation with FMC so the larger buffer scales (4, 6, 8, 10 m) were omitted. Similarly, we retained the 6-day cumulative precipitation window as it had the strongest Pearson correlation with FMC. Cumulative precipitation windows with weaker correlations (5 and 11 h; 35 h; and 3, 9, 12, 15, 18 and 21 day) were omitted.

Results

FMC spatial variability

There is a trend towards wetter and more spatially variable FMC values during observation days through the midsummer period and drier and less variable values during the early and late-summer periods (Fig. 3a). The early, mid and late summer median FMC values were 9, 34 and 14%, respectively (Table 1). The early, mid and later summer standard deviation values were 22, 35 and 17% while the ranges of FMC spanned 193, 302 and 142% during these three intraseasonal periods (Table 1). During the early and late summer periods, 14 and 19% of observations were greater than the 30% moisture of extinction, a rule of thumb threshold above which flaming combustion cannot occur, whereas during the mid-summer period, 55% of observations were greater than 30% (Table 1; Fig. 3c). Over the 2022 fire season, the skewness values of the three periods decreased from 3.43 in the early summer to 2.61 during the mid-summer period and 2.45 during the late summer period (Table 1). The positive values indicate righttailed distributions through all periods. The first sampling

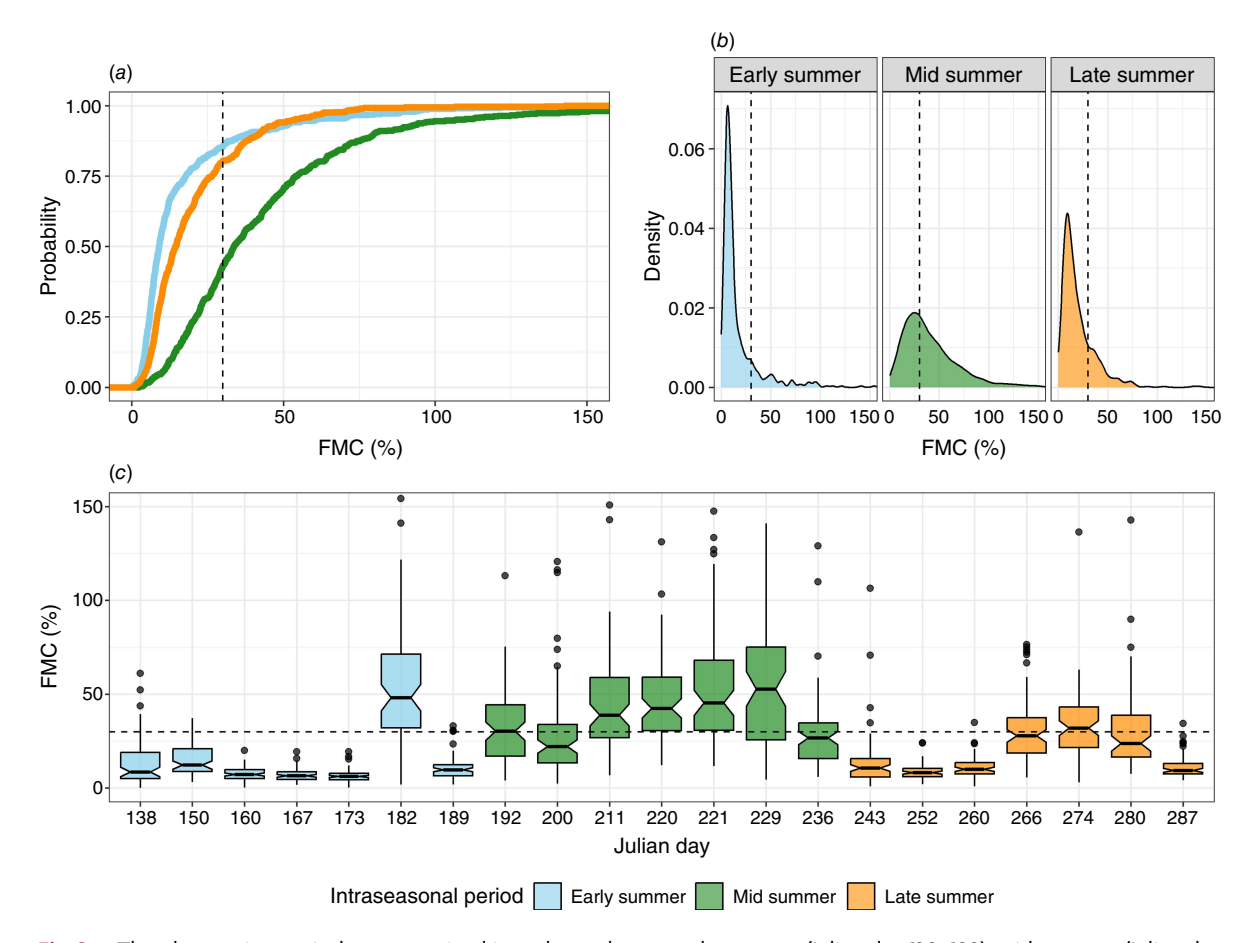


Fig. 3. The observation period was organized into three phases: early summer (Julian day 138–189), mid-summer (Julian day 192–236) and late summer (Julian day 243–287) for the following plots. The dashed lines on the axes depicting FMC indicate the commonly used 30% moisture of extinction threshold for dead understory forest fuels (Rothermel et al. 1986). (a) Empirical cumulative density functions of the three distributions (early summer, mid-summer, late summer) of observed fuel moisture content. (b) Kernel density plots of the three intraseasonal period distributions. (c) Boxplots colored by intraseasonal period depicting the distribution of FMC on each observation day. The box indicates the inter-quartile range (25th to 75th percentiles). The mid-band indicates the median, and the whiskers indicate points within 1.5 times the interquartile range. Points outside the whiskers are outliers. Note: to visualize the data more effectively, the axes depicting FMC (%) were visually constrained to 150%, preserving all values while focusing on a more relevant range.

Table 1. Summary statistics of FMC.

Period	Mean (%)	Median (%)	s.d. (%)	Skewness	Kurtosis	Observations over 30% (%)
Early summer	17	9	22	3.43	15.64	14
Mid summer	43	34	35	2.61	10.79	55
Late summer	20	14	17	2.45	9.83	19

Summary statistics with the observation period organized into thirds, early summer (Julian day 138–189), mid-summer (Julian day 192–236) and late summer (Julian day 243–287).

period also has the greatest kurtosis value of 15.6, indicating the 'peakiest' distribution compared with the kurtosis values during the mid-summer and late summer periods of 10.7 and 9.83 (Table 1; Fig. 3b).

Of the tested spatiotemporal model forms, a sum-metric model provided the best fit (Table 2). The model structure shows that approximately 85% of the semivariance in space

occurs in the first 10 m and \sim 80% of the semivariance in time happens in the first 20 days from a sample point (Fig. 4). Additionally, the nugget values for the spatial, temporal and joint components were 0, 349.93 and 224.16, respectively (Table 2), where the temporal nugget accounts for \sim 66% of variation across time but the joint nugget shrinks to account for <5% of variation in the

Table 2. Spatiotemporal variogram model parameters.

Component	Nugget	Sill	Range
Space	0	1006.07	987.85
Time	349.93	524.40	82.85
Joint	224.16	5035.43	63.51

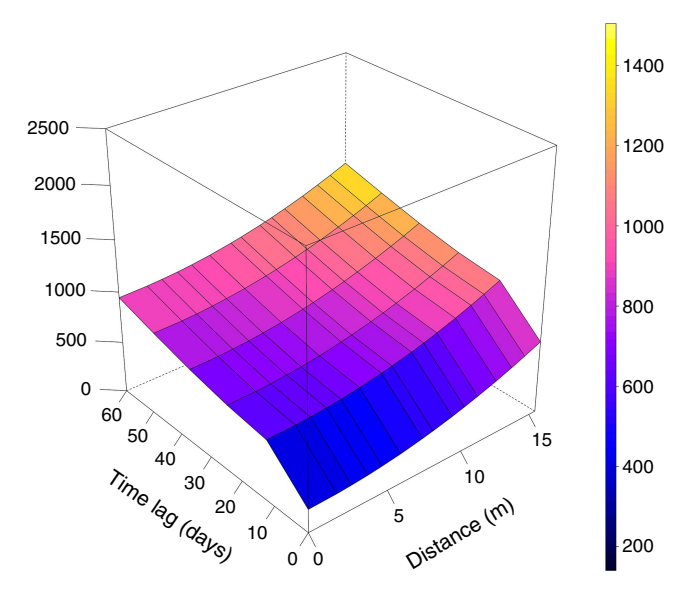


Fig. 4. Spatiotemporal fitted variogram model using a sum-metric approach. The wireframe plot represents the estimated semivariance on the vertical axis as a function of spatial distance (m) and temporal lag (days). The model accounts for spatial, temporal and joint spatiotemporal dependencies.

combined dynamics. The interpolated values in the ordinary kriging approach indicate a larger range in FMC values during the wetter, mid-summer days versus the drier early-summer days (Fig. 5). Similarly, the kriged maps show more spatially homogeneous FMC values during the early summer and more heterogeneous values during the mid-summer and late summer periods (Fig. 5). Additionally, several areas exhibit persistent fuel moisture, maintaining relatively stable dry or wet conditions across multiple kriged days.

Environmental control effect on FMC

The GAM explained 35.4% of the deviance in FMC with an adjusted R^2 of 0.33. The smoothed terms, understory cover, canopy cover at the 2 m radius, heat load index and 6-day cumulative precipitation all showed statistically significant associations with FMC (P < 0.001, P < 0.001, P < 0.006, P < 0.001, respectively; Table 3). The interactions between understory cover, canopy cover and heat load index with precipitation did not display significant associations with FMC (Table 3).

The relationship between understory cover and FMC shows that as understory cover increases, FMC also rises.

Specifically, expected FMC increases from $\sim 10\%$ at the lowest levels of understory cover to $\sim 18\%$ at the highest levels, following an exponential curve (Fig. 6a). Canopy cover has a weak positive correlation with FMC, with expected values increasing from approximately 11 to 16% (Fig. 6b). Heat load index and expected FMC have a negative relationship with FMC, decreasing from ~ 16 to 12% (Fig. 6c). Precipitation has a strong positive, though non-linear, association with FMC ranging from $\sim 15\%$ FMC at lower precipitation values to $\sim 50\%$ at the highest precipitation values. Expected FMC peaks at $\sim 70\%$ and 35 mm of precipitation in an area of substantial model uncertainty.

Discussion

Fine dead FMC shows exceptional fine-scale variability within forest stands, driven by sub-seasonal precipitation patterns. FMC was low in the early and late summer periods and high in the mid-summer period. In contrast to the early and late summer periods, frequent, intense precipitation events, driven by the North American monsoon, increased the mean and within-stand variability of FMC observations during the mid-summer period. For example, during the mid-summer period, 55% of FMC observations were greater than the 30% moisture of extinction threshold. In contrast, the lowest spatial variability in FMC occurred during the early summer intraseasonal period, when just 14% of observations were greater than 30% (Table 1). Notably, 13% of the observations greater than 30% were recorded on just a single day (Julian day 182), the day after a particularly large rainfall event. This suggests that precipitation events not only increase mean FMC but introduce heterogeneity through local-scale variations in vegetation structure, topography and micrometeorological processes. Because fine dead fuels form a major component of available fuels for surface fire spread in frequent-fire systems (Anderson 1981; Mitchell et al. 2009), this within-stand variability indicates the potential for differential fire spread throughout a stand, perhaps most notable during relatively wet intraseasonal periods.

Our findings indicate that fine-scale environmental controls, including vegetation structure and topography, moderate the larger-scale effect of sub-seasonal precipitation patterns. Canopy cover and understory cover are positively associated with FMC. This finding suggests that denser vegetation structures limit solar insolation to the understory, creating cooler and damper conditions at the fuel interface, consistent with findings by Pickering *et al.* (2021) and Kreye *et al.* (2018). We also found a negative correlation between heat load index and FMC that aligns with previous research, indicating that pole-facing slopes support moister conditions, driven by differences in solar radiative heating (Stambaugh *et al.* 2007; Nyman *et al.* 2015; Slijepcevic *et al.* 2018). However, our findings differ from those of

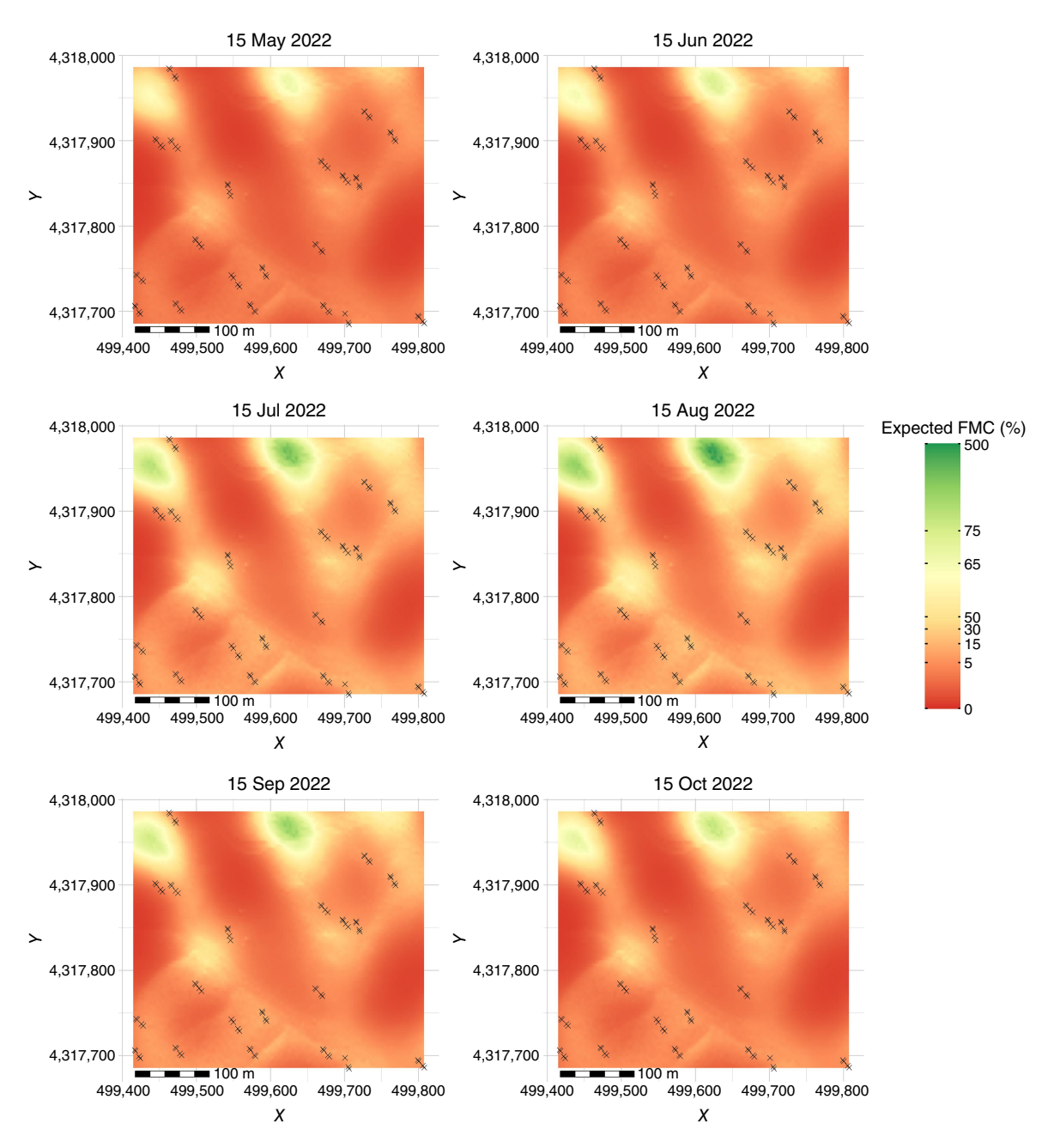


Fig. 5. Kriged fuel moisture content predictions on the 15th day of each observation month. A square-root transformation was applied to the predicted FMC values prior to color mapping to improve contrast in the lower, fire behavior-relevant FMC range. Values shown on the color scale were back-transformed to percentage FMC for interpretability. Sampling locations are depicted with diagonal crosses.

Gibos (2010) who reported minimal aspect-related variation in FMC within dense canopy lodgepole pine (*Pinus contorta*) stands in Alberta, Canada. At our site, where post-treatment canopy cover is relatively low, pole-facing slopes retained higher fuel moisture values. Our findings, along with others (Nyman *et al.* 2015; Slijepcevic *et al.* 2018; Pickering *et al.* 2021), indicate that differences in solar insolation driven by

heterogeneity in cover and topography underlie the spatial variation of fine dead FMC.

At the within-stand scale, canopy cover, understory cover and topography influenced FMC independently of cumulative precipitation over the 6 days preceding each FMC observation. In contrast, studies at coarser stand scales report the effect of vegetation structure on FMC appears to

Table 3. Generalized additive model summary.

Family	Link function	Formula	Adjusted R ²	Deviance explained (%)
Gamma	log	FMC ~ s(u_cover) + s(c_cover) + s(hli) + s (precip) + ti(u_cover:precip) + ti (c_cover:precip) + ti(hli:precip)	0.33	35.4
	Estimate	Standard error	T value	Pr(> z)
Intercept	3.12	0.021	144.7	<0.001
	Effective degrees of freedom (ed.f.)	Reference degrees of freedom (Ref.d.f.)	F statistic	Pr(> z)
u_cover	1.47	1.81	28.95	<0.001
c_cover	8.14	1	16.36	<0.001
hli	1.21	1.39	7	0.006
precip	8.14	8.74	58.65	<0.001
u_cover:precip	3.03	4.26	1.28	0.269
c_cover:precip	1.56	1.87	0.48	0.662
hli:precip	2.62	3.05	1.97	0.115

Spatiotemporal variogram nugget, sill and range values of the fitted model are specified for the space, time and joint space time component models (extracted using the extractPar function in the gstat package).

Generalized additive model summary with the smoothed main effects of understory cover (u_cover), canopy cover (c_cover), heat load index (hli), precipitation (precip) and the interaction terms of understory cover, canopy cover and heat load index with precipitation.

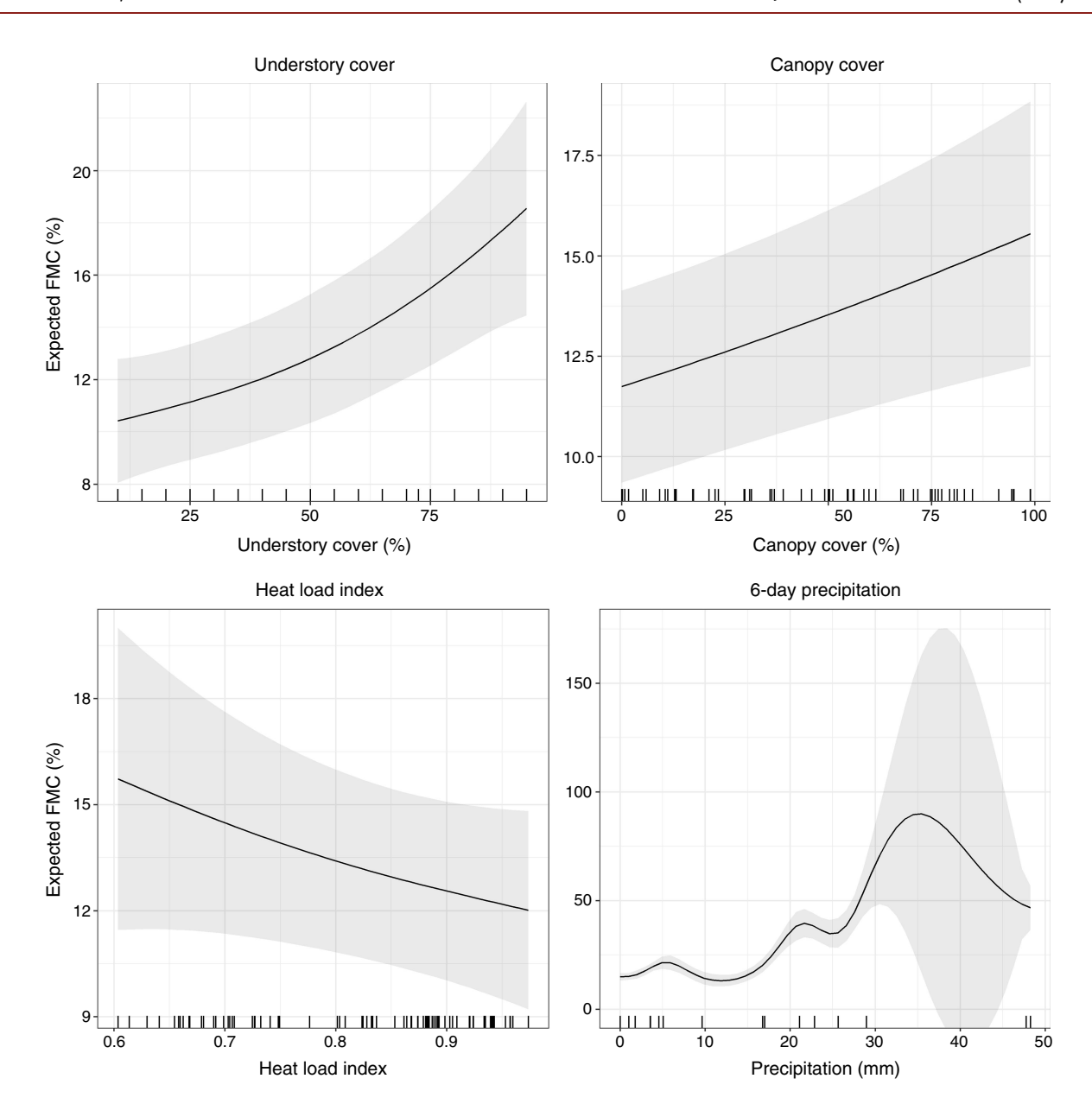


Fig. 6. The smoothed, marginal effects of understory cover, canopy cover, heat load index and precipitation on FMC transformed to show the fitted GAM function on the response scale. The *x* axis shows values of the covariate, the rug indicates the distribution of covariate observations, and the *y* axis shows expected FMC values. The gray bands correspond to the 95% confidence interval and represent model uncertainty in the transformed (response scale) estimate. Though negative values are not possible in FMC or under a Gamma distribution, the confidence interval below 0 in the precipitation plot is an artifact of transformation and reflects wide uncertainty.

depend on the broader, regional moisture regime (e.g. coastal fog; Kane 2021), a relationship not observed at finer scales. If there is indeed an interaction between vegetation structure and larger-scale moisture regime in the semi-arid climate being evaluated, it is likely due to the specific metric used or the timing of the FMC observations relative to the measured precipitation events. Alternative variables such as evapotranspiration or climatic moisture deficit may be better suited to detect it. Additionally, this potential interaction may be somewhat short-lived. Although the 6-day cumulative precipitation

shows the strongest Pearson correlation with FMC, the interactive effect with forest structural variables may no longer be detectable over such a broad temporal window. The insignificant interactions in the GAM suggest that finer-scale interactions between vegetation structure and moisture regimes may be transient and context-dependent, requiring more precise temporal sampling or alternative environmental variables to fully capture their influence on FMC.

FMC values exhibit patterns of spatiotemporal autocorrelation across the scales in which we sampled. According to the joint space-time variogram (Fig. 4), ~80% of the observed semivariance occurs at spatial scales finer than 15 m. The nugget values in the temporal and joint spatiotemporal model components reflect variations in FMC at temporal lag distances finer than the sampling interval (approximately weekly), confirming that fine fuels respond to atmospheric conditions at finer scales. Although previous research has evaluated patterns of spatial autocorrelation in FMC (Zhang et al. 2021) and temporal trends in FMC over both seasonal (Faiella and Bailey 2007; Kane 2021) and diel scales (Banwell et al. 2013), to the best of our knowledge, there have been no studies to investigate autocorrelation over spatiotemporal scales. Consistent with Zhang et al. (2021), who observed anisotropic spatial autocorrelation patterns of FMC at scales of 3.5-5.5 m in a larch forest in China, our results demonstrate spatial variability at similarly fine scales. These fine-scale variations in FMC are likely driven by the aggregated tree spacing within the stand, microtopography and other fine-scale spatial variability of vegetation or environmental parameters. For instance, shrub, dead woody and litter fuel loading (Vakili et al. 2016) and soil moisture (Comegna and Basile 1994; Anctil et al. 2002; Brocca et al. 2007) are shown to vary at similar fine scales (approximately 1–5 m). Additionally, this spatial variability is inconsistent over time, potentially driven by varying moisture adsorption through precipitation mediated by vegetation structure (Crockford Richardson 2000; Thomas 2016; Kreye et al. 2018) nocturnal moisture recovery (Holden and Jolly 2011).

The distribution of FMC observations at within-stand scales included values both above and below 30% on 18 of the 21 sampling days, indicating a mixture of burnable and non-burnable areas at fine spatial scales. This spatial discontinuity in fuels available for ignition could influence wildland fire spread, fire sustainability and spot-fire hazard (Koo et al. 2010; Wang et al. 2024). Additionally, because most prescribed fires are ignited under marginal conditions (Hiers et al. 2020), understanding the magnitude of fuel moisture variability during these relatively wet conditions may be crucial for informing and achieving management objectives (Bonner et al. 2024). The application of prescribed fire under marginal, more spatially variable conditions likely increases the heterogeneity of severities, which support ecological objectives (Parr and Brockett 1999; Robertson et al. 2019). In contrast, applying prescribed fire under more homogeneously dry conditions may be better suited for fuels reduction - though other variables related to topography and weather are critical for predicting fire behavior and severity (Rothermel 1972).

Because fine dead fuels adsorb and desorb moisture fairly quickly (Fosberg *et al.* 1970), a limitation of the present study is the potential conflation of temporal and spatial variability. On each observation day, we sampled FMC from plots in a consistent order over a ~1.5-h period. Although this sampling method maximized efficiency, it is

possible that over this ~1.5-h period, moisture contents fluctuated in response to changing atmospheric conditions. However, we consider this effect to be minor as prior research indicates that ponderosa pine needles – the dominant fuel in our study – have a moisture time lag of approximately 4 h (Fosberg 1975; Anderson *et al.* 1978). This suggests that substantial shifts in FMC over a 1.5-h window are unlikely. Future work would benefit from more tightly constrained sampling windows and should aim to better characterize diel fluctuations in fine, *in situ* fuels.

Given the complicated interaction of FMC across space and time, further research is needed to better understand how within-stand moisture variability responds to the full suite of environmental controls such as varying weather, soil and topographic conditions, and vegetation structure. Advancing this understanding can inform prescribed fire ignition planning and improve predictions of resulting fire behavior and spread. Laboratory and in situ wildland fire experiments as well as numerical simulations are well suited to investigate the potential impact of spatial variability in moisture content on fire behavior, especially as increased attention is given to sub-grid processes in fire behavior modeling (Marshall et al. 2023) and controlled experiments adopt precise instrumentation (Prichard et al. 2019). Considering the full spatial variability of FMC may enhance our ability to predict fire behavior more accurately, optimize prescribed fire applications and achieve both ecological and fuel management objectives more effectively.

References

Anctil F, Mathieu R, Parent LÉ, Viau AA, Sbih M, Hessami M (2002) Geostatistics of near-surface moisture in bare cultivated organic soils. *Journal of Hydrology* **260**(1–4), 30–37. doi:10.1016/S0022-1694(01) 00600-X

Anderson HE (1981) 'Aids to Determining Fuel Models for Estimating Fire Behavior. Vol. 122.' (USDA Forest Service, Intermountain Forest and Range Experiment Station)

Anderson HE, Schuette RD, Mutch RW (1978) 'Timelag and Equilibrium Moisture Content of Ponderosa Pine Needles. Vol. 202.' (USDA Forest Service, Intermountain Forest and Range Experiment Station)

Banwell EM, Varner M, Knapp EE, van Kirk RW (2013) Spatial, seasonal, and diel forest floor moisture dynamics in Jeffrey pine-white fir forests of the Lake Tahoe Basin, USA. Forest Ecology and Management 305, 11–20. doi:10.1016/j.foreco.2013.05.005

Biddulph J, Kellman M (1998) Fuels and fire at savanna–gallery forest boundaries in southeastern Venezuela. *Journal of Tropical Ecology* **14**(4), 445–461. doi:10.1017/S0266467498000339

Bonner SR, Hoffman CM, Linn RR, Tinkham WT, Atchley AL, Sieg CH, Varner JM, O'Brien JJ, Hiers JK (2024) Forest structural complexity and ignition pattern influence simulated prescribed fire effects. *Fire Ecology* **20**(1), 82. doi:10.1186/s42408-024-00314-7

Bradford MA, Veen G, Bonis A, Bradford EM, Classen AT, Cornelissen JHC, Crowther TW, De Long JR, Freschet GT, Kardol P, Manrubia-Freixa M, Maynard DS, Newman GS, Logtestijn R, Viketoft M, Wardle DA, Wieder WR, Wood SA, van der Putten WH (2017) A test of the hierarchical model of litter decomposition. *Nature Ecology & Evolution* 1(12), 1836–1845. doi:10.1038/s41559-017-0367-4

Bradshaw LS and McCormick E (2000) 'Fire Family Plus User's Guide.' (USDA Forest Service, Rocky Mountain Research Station: Fort Collins, CO)

Bradshaw LS, Deeming JE, Burgan RE, Jack D (1984) The 1978 National Fire-Danger Rating System: Technical Documentation. Vol.

- 169'. 44 p. General Technical Report INT-169. (USDA Forest Service, Intermountain Forest and Range Experiment Station: Ogden, UT)
- Brocca L, Morbidelli R, Melone F, Moramarco T (2007) Soil moisture spatial variability in experimental areas of central Italy. Journal of Hydrology 333(2–4), 356–373. doi:10.1016/j.jhydrol. 2006.09.004
- Burrows ND (1999) Fire behaviour in jarrah forest fuels: 2. Field experiments. *CALMScience* 3(1), 57–84. Available at https://www.cabidigitallibrary.org/doi/full/10.5555/19990603025
- Cannon JB, Tinkham WT, DeAngelis RK, Hill EM, Battaglia MA (2019) Variability in mixed conifer spatial structure changes understory light environments. *Forests* **10**(11), 1015. doi:10.3390/f10111015
- Cawson JG, Burton JE, Pickering BJ, Penman TD (2024) Moisture thresholds for ignition vary between types of eucalypt forests across an aridity gradient. *Landscape Ecology* **39**(3), 70. doi:10.1007/s10980-024-01864-6
- Churchill DJ, Larson AJ, Dahlgreen MC, Franklin JF, Hessburg P, Lutz JA (2013) Restoring forest resilience: from reference spatial patterns to silvicultural prescriptions and monitoring. *Forest Ecology and Management* **291**, 442–457. doi:10.1016/j.foreco.2012.11.007
- Comegna V, Basile A (1994) Temporal stability of spatial patterns of soil water storage in a cultivated Vesuvian soil. *Geoderma* **62**(1–3), 299–310. doi:10.1016/0016-7061(94)90042-6
- Crawford AJ, Belcher CM, Morison JI, Doerr SH, Kettridge N, Clay GD (2025) Fuel moisture and flammability of leaf litter in British forest plantations and their implications for wildfire risk. *Forestry* cpaf029. doi:10.1093/forestry/cpaf029
- Crockford RH, Richardson DP (2000) Partitioning of rainfall into throughfall, stemflow and interception: effect of forest type, ground cover and climate. *Hydrological Processes* **14**(16–17), 2903–2920. doi:10.1002/1099-1085(200011/12)14:16/17 < 2903::AID-HYP126 > 3. 0.CO;2-6
- Diószegi G, Immitzer M, Müller MM, Vacik H (2023) Effects of interaction between forest structure and precipitation event characteristics on fuel moisture conditions. *Agricultural and Forest Meteorology* **342**, 109681. doi:10.1016/j.agrformet.2023.109681
- Ellis TM, Bowman D, Jain P, Flannigan MD, Williamson GJ (2022) Global increase in wildfire risk due to climate-driven declines in fuel moisture. *Global Change Biology* **28**(4), 1544–1559. doi:10.1111/gcb.16006
- Estes BL, Knapp EE, Skinner CN, Uzoh FC (2012) Seasonal variation in surface fuel moisture between unthinned and thinned mixed conifer forest, northern California, USA. *International Journal of Wildland Fire* **21**(4), 428–435. doi:10.1071/WF11056
- Faiella SM, Bailey JD (2007) Fluctuations in fuel moisture across restoration treatments in semi-arid ponderosa pine forests of northern Arizona, USA. *International Journal of Wildland Fire* **16**(1), 119–127. doi:10.1071/WF06018
- Fernandes PM, Botelho H, Rego F, Loureiro C (2008) Using fuel and weather variables to predict the sustainability of surface fire spread in maritime pine stands. *Canadian Journal of Forest Research* **38**(2), 190–201. doi:10.1139/X07-159
- Fosberg MA (1975) 'Heat and Water Vapor Flux in Conifer Forest Litter and Duff: A Theoretical Model, Vol. 152.' (USDA Forest Service, Rocky Mountain Forest and Range Experiment Station)
- Fosberg MA, Lancaster JW, Schroeder MJ (1970) Fuel moisture response—drying relationships under standard and field conditions. *Forest Science* **16**(1), 121–128. doi:10.1093/forestscience/16.1.121
- Gibos KE (2010) Effect of slope and aspect on litter layer moisture content of lodgepole pine stands in the eastern slopes of the Rocky Mountains of Alberta. Doctoral Dissertation, University of Toronto, Ontario, Canada.
- Gräler B, Pebesma EJ, Heuvelink G (2016) Spatio-temporal interpolation using gstat. *The R Journal* 8(1), 204–218. doi:10.32614/RJ-2016-014
- Hardwick SR, Toumi R, Pfeifer M, Turner EC, Nilus R, Ewers RM (2015)
 The relationship between leaf area index and microclimate in tropical forest and oil palm plantation: forest disturbance drives changes in microclimate. *Agricultural and Forest Meteorology* **201**, 187–195. doi:10.1016/j.agrformet.2014.11.010
- Hastie TJ (2017) Generalized additive models. In 'Statistical models in S'. (Ed. TJ Hastie) pp. 249–307. (Routledge)

- Hiers JK, Staudhammer CL, O'Brien J, Gholz HL, Martin TA, Hom J, Starr G (2019) Fine dead fuel moisture shows complex lagged responses to environmental conditions in a saw palmetto (*Serenoa repens*) flatwoods. *Agricultural and Forest Meteorology* **266**, 20–28. doi:10.1016/j.agrformet.2018.11.038
- Hiers JK, O'Brien JJ, Varner JM, Butler BW, Dickinson M, Furman J, Gallagher M, Godwin D, Goodrick SL, Hood SM, Hudak A (2020) Prescribed fire science: the case for a refined research agenda. *Fire Ecology* **16**, 1–15. doi:10.1186/s42408-020-0070-8
- Hoffman CM, Ziegler JP, Tinkham WT, Hiers JK, Hudak AT (2023) A comparison of four spatial interpolation methods for modeling fine-scale surface fuel load in a mixed conifer forest with complex terrain. *Fire* **6**(6), 216. doi:10.3390/fire6060216
- Holden ZA, Jolly WM (2011) Modeling topographic influences on fuel moisture and fire danger in complex terrain to improve wildland fire management decision support. *Forest Ecology and Management* **262**(12), 2133–2141. doi:10.1016/j.foreco
- Hood PR, Nelson KN, Rhoades CC, Tinker DB (2017) The effect of salvage logging on surface fuel loads and fuel moisture in beetle-infested lodgepole pine forests. *Forest Ecology and Management* **390**, 80–88. doi:10.1016/j.foreco.2017.01.003
- Jurdao S, Chuvieco E, Arevalillo JM (2012) Modelling fire ignition probability from satellite estimates of live fuel moisture content. *Fire Ecology* **8**, 77–97. doi:10.4996/fireecology.0801077
- Kane JM (2021) Stand conditions alter seasonal microclimate and dead fuel moisture in a northwestern California oak woodland. Agricultural and Forest Meteorology 308, 108602. doi:10.1016/j.agrformet.2021. 108602
- Knapp EE, Keeley JE (2006) Heterogeneity in fire severity within early season and late season prescribed burns in a mixed-conifer forest. *International Journal of Wildland Fire* **15**(1), 37–45. doi:10.1071/WE04068
- Koo E, Pagni PJ, Weise DR, Woycheese JP (2010) Firebrands and spotting ignition in large-scale fires. *International Journal of Wildland Fire* 19(7), 818–843. doi:10.1071/WF07119
- Kreye JK, Hiers JK, Varner JM, Hornsby B, Drukker S, O'brien JJ (2018) Effects of solar heating on the moisture dynamics of forest floor litter in humid environments: composition, structure, and position matter. *Canadian Journal of Forest Research* **48**(11), 1331–1342. doi:10.1139/cjfr-2018-0147
- Kuo M, Cox SK (1975) Analysis of Colorado precipitation. Completion Report Series 63. Available at https://api.mountainscholar.org/ server/api/core/bitstreams/b342fde6-3fe4-4346-971a-1b019d0011b7/ content
- LANDFIRE (2020) LANDFIRE fire return interval. Available at https://landfire.gov/fri.php [accessed 8 December 2023]
- Linn R, Reisner J, Colman JJ, Winterkamp J (2002) Studying wildfire behavior using FIRETEC. *International Journal of Wildland Fire* 11(4), 233–246. doi:10.1071/WF02007
- Little K, Graham LJ, Flannigan M, Belcher CM, Kettridge N (2024) Landscape controls on fuel moisture variability in fire-prone heathland and peatland landscapes. *Fire Ecology* **20**(1), 14. doi:10.1186/s42408-024-00248-0
- Liu Y (2017) Responses of dead forest fuel moisture to climate change. Ecohydrology 10(2), e1760. doi:10.1002/eco.1760
- Loudermilk EL, O'Brien JJ, Mitchell RJ, Cropper WP, Hiers JK, Grunwald S, Grego J, Fernandez-Diaz JC (2012) Linking complex forest fuel structure and fire behaviour at fine scales. *International Journal of Wildland Fire* 21(7), 882–893. doi:10.1071/WF10116
- Marshall GA, Linn RR, Holmes M, Goodrick S, Thompson DK, Hemmati A (2023) Capturing sub-grid temperature and moisture variations for wildland fire modeling. *Environmental Modelling & Software* **164**, 105678.
- Matthews S (2010) Effect of drying temperature on fuel moisture content measurements. *International Journal of Wildland Fire* **19**(6), 800–802. doi:10.1071/WF08188
- McArthur AG (1967) Fire behaviour in Eucalypt forests. Commonwealth of Australia, Forestry and Timber Bureau Leaflet 107. (Canberra, ACT)
- McCune B, Keon D (2002) Equations for potential annual direct incident radiation and heat load. *Journal of Vegetation Science* **13**(4), 603–606. doi:10.1111/j.1654-1103.2002.tb02087.x

- Mitchell RJ, Hiers JK, O'Brien J, Starr G (2009) Ecological forestry in the Southeast: understanding the ecology of fuels. *Journal of Forestry* **107**(8), 391–397. doi:10.1093/jof/107.8.391
- Moon K, Duff TJ, Tolhurst KG (2013) Characterizing forest wind profiles for utilization in fire spread models. In 'Twentieth International Congress on Modelling and Simulation'. Adelaide, Australia.
- Nyman P, Metzen D, Noske PJ, Lane PNJ, Sheridan GJ (2015) Quantifying the effects of topographic aspect on water content and temperature in fine surface fuel. *International Journal of Wildland Fire* **24**(8), 1129–1142. doi:10.1071/WF14195
- O'Rourke S, Kelly GE (2015) Spatio-temporal modelling of forest growth spanning 50 years—the effects of different thinning strategies. *Procedia Environmental Sciences* **26**, 101–104. doi:10.1016/j.proenv. 2015.05.008
- Parr CL, Brockett BH (1999) Patch-mosaic burning: a new paradigm for savanna fire management in protected areas? *Koedoe* **42**(2), 117–130. doi:10.4102/koedoe.v42i2.237
- Pebesma E, Bivand R (2005) Classes and methods for spatial data in R. *R News* 5(2), 9–13. Available at https://CRAN.R-project.org/doc/Rnews/Pebesma E, Bivand R (2023) 'Spatial Data Science: With Applications in R.' (Chapman and Hall/CRC) doi:10.1201/9780429459016
- Pebesma EJ (2004) Multivariable geostatistics in S: the gstat package. Computers & Geosciences 30, 683-691.
- Pedersen EJ, Miller DL, Simpson GL, Ross N (2019) Hierarchical generalized additive models in ecology: an introduction with mgcv. *PeerJ* **7**, e6876. doi:10.7717/peerj.6876
- Pickering BJ, Duff TJ, Baillie C, Cawson JG (2021) Darker, cooler, wetter: forest understories influence surface fuel moisture. *Agricultural and Forest Meteorology* **300**, 108311. doi:10.1016/j.agrformet.2020.108311
- Prichard S, Larkin NS, Ottmar R, French N, Baker K, Brown T, Clements C, Dickinson M, Hudak A, Kochanski A, Linn R, Liu Y, Potter B, Mell W, Tanzer D, Urbanski S, Watts A (2019) The fire and smoke model evaluation experiment—a plan for integrated, large fire—atmosphere field campaigns. *Atmosphere* 10(2), 66. doi:10.3390/atmos10020066
- PRISM Climate Group (2020) 'PRISM Climate Group 2020.' (Oregon State University: Corvallis, OR) Available at http://prism.oregon state.edu [accessed 3 July 2024]
- R Core Team (2024) R: A Language and Environment for Statistical Computing. (R Foundation for Statistical Computing: Vienna, Austria) Available at https://www.R-project.org/
- Robertson KM, Platt WJ, Faires CE (2019) Patchy fires promote regeneration of longleaf pine (*Pinus palustris* Mill.) in pine savannas. *Forests* **10**(5), 367. doi:10.3390/f10050367
- Rothermel RC (1972) 'A Mathematical Model for Predicting Fire Spread in Wildland Fuels. Vol. 115.' (USDA Forest Service, Intermountain Forest & Range Experiment Station)
- Rothermel RC, Wilson RA, Morris GA, Sackett SS (1986) 'Modeling Moisture Content of Fine Dead Wildland Fuels.' (USDA Forest Service, Intermountain Forest and Range Experiment Station)
- Ryan KC, Knapp EE, Varner JM (2013) Prescribed fire in North American forests and woodlands: history, current practice, and challenges. Frontiers in Ecology and the Environment 11(1), e15–e24. doi:10.1890/120329

- Schoennagel T, Veblen TT, Romme WH, Sibold JS, Cook ER (2005) ENSO and PDO variability affect drought-induced fire occurrence in Rocky Mountain subalpine forests. *Ecological Applications* **15**(6), 2000–2014. doi:10.1890/04-1579
- Sherriff RL, Veblen TT (2008) Variability in fire-climate relationships in ponderosa pine forests in the Colorado Front Range. *International Journal of Wildland Fire* 17(1), 50–59. doi:10.1071/WF07029
- Slijepcevic A, Anderson WR, Matthews S, Anderson DH (2018) An analysis of the effect of aspect and vegetation type on fine fuel moisture content in eucalypt forest. *International Journal of Wildland Fire* **27**(3), 190–202. doi:10.1071/WF17049
- Snepvangers JJJC, Heuvelink GBM, Huisman JA (2003) Soil water content interpolation using spatio-temporal kriging with external drift. *Geoderma* **112**(3–4), 253–271. doi:10.1016/S0016-7061(02) 00310-5
- Stambaugh MC, Guyette RP, Dey DC (2007) Forest fuels and landscapelevel fire risk assessment of the Ozark Highlands, Missouri. e-General Technical Report SRS-101. pp. 258–266. (USDA Forest Service, Southern Research Station)
- Tanskanen H, Granström A, Venäläinen A, Puttonen P (2006) Moisture dynamics of moss-dominated surface fuel in relation to the structure of *Picea abies* and *Pinus sylvestris* stands. *Forest Ecology and Management* **226**(1–3), 189–198. doi:10.1016/j.foreco.2006.01.048
- Thomas S (2016) 'Differences in Rainfall Interception Losses for Three Tree Species Common to Colorado: *Populus tremuloides, Picea engelmannii,* and *Pinus ponderosa.*' (University of Colorado Colorado Springs)
- Turner MG, Romme WH (1994) Landscape dynamics in crown fire ecosystems. Landscape Ecology 9, 59–77. doi:10.1007/BF00135079
- United States Geological Survey (2021) United States Geological Survey 3D Elevation Program 1 Meter Digital Elevation Model. Distributed by OpenTopography. doi:10.5069/G98K778D
- Vakili E, Hoffman CM, Keane RE, Tinkham WT, Dickinson Y (2016) Spatial variability of surface fuels in treated and untreated ponderosa pine forests of the southern Rocky Mountains. *International Journal of Wildland Fire* **25**(11), 1156–1168. doi:10.1071/WF16072
- Veblen TT, Kitzberger T, Donnegan J (2000) Climatic and human influences on fire regimes in ponderosa pine forests in the Colorado Front Range. *Ecological Applications* **10**(4), 1178–1195. doi:10.1890/1051-0761(2000)010[1178:CAHIOF]2.0.CO;2
- Viney NR (1991) A review of fine fuel moisture modelling. *International Journal of Wildland Fire* 1(4), 215–234. doi:10.1071/WF9910215
- Wagner CV (1987) 'Development and structure of the Canadian Forest Fire Weather Index system.' (No. 35, pp. viii+-37) Retrieved from http://cfs.nrcan.gc.ca/publications?id=19927
- Wang S, Thomsen M, Huang X, Fernandez-Pello C (2024) Spot ignition of a wildland fire and its transition to propagation. *International Journal of Wildland Fire* 33(7), WF23207. doi:10.1071/WF23207
- Wood SN (2017) 'Generalized Additive Models: An Introduction with R.' 2nd edn. (Chapman and Hall/CRC)
- Zhang H, Ma S, Kang P, Zhang Q, Wu Z (2021) Spatial heterogeneity of dead fuel moisture content in a *Larix gmelinii* forest in Inner Mongolia using geostatistics. *Journal of Forestry Research* **32**(2), 569–577. doi:10.1007/s11676-020-01167-x

Data availability. The data supporting this research will be made available on reasonable request to the corresponding author.

Conflicts of interest. The authors declare no conflicts of interest.

Declaration of funding. This research was funded under the Department of Defense Strategic Environmental Research and Development Program grant RC19 – 1119.

Acknowledgements. The authors would like to thank Kate Johnston, Lauren Lad, Rick Grybko, Lydia Hoffman, Casey Menick, Jamie Woolet and Katarina Warnick for help in sample collection and processing. The authors are also thankful to the Pike San Isabel National Forest for study site access and the Woodland Park Public Library for access to their facilities for sample processing. The findings and conclusions in this publication are those of the authors and should not be construed to represent any official USDA or US Government determination or policy.

Author affiliations

- ^ADepartment of Forest and Rangeland Stewardship, Colorado State University, Fort Collins, CO, USA.
- ^BRocky Mountain Research Station, United States Department of Agriculture, Forest Service, Fort Collins, CO, USA.
- CNatural Resources Institute, Texas A&M University-Washington, DC, USA.

Appendix 1. Overstory and understory summary statistics

The below post-treatment summary statistics have been extracted from 0.04 ha (1/10th acre) polygons around each fuel moisture plot (n = 80).

	Mean	s.d.	Min.	Max.
Trees per hectare	358	272	25	1186
Basal area (m² ha ⁻¹)	12.8	4.9	2.6	23.9
Mean height (m)	12.4	4.2	6.0	20.2
Mean crown base height (m)	6.7	2.7	2.0	12.1

The understory cover data below is from a pre-treatment monitoring effort within the Pikes Peak Forest Dynamics Plot. Note the understory data were collected from plots distinct from those in the present study (W. Tinkham, unpublished data, 2025).

Below are the five most common species found: *Carex* spp. (sedges), *Juniperus communis* (common juniper), *Fragaria virginiana* (Virginia strawberry), *Achillea millefolium* (yarrow) and *Allium cernuum* (nodding onion).

Species	% of plots	Mean cover (%)
Sedge	65.1	5.0
Common juniper	34.0	26.3
Virginia strawberry	29.0	4.4
Yarrow	24.0	4.0
Nodding onion	24.0	3.7

Appendix 2. Site-specific crown diameter allometric equations

Crown diameter was predicted based on a sample of 467 tree observations collected in the site by randomly sampling 16 of the 20×20 m grid cells. Species-specific prediction models were built using a linear regression with tree DBH and height as predictors. Models were reduced to minimize the Akaike Information Criterion resulting in the below relationships. Sampled species include PIPO (*Pinus ponderosa* P. and C. Lawson), PIEN (*Picea engelmannii* Parry ex. Engelman), PIFL (*Pinus flexilis* James), PIPU (*Picea pungens* Engelm.), POTR (*Populus tremuloides* Michx.) and PSME (*Pseudotsuga menziesii* Mirb).

Species	n	Adj R²	RSE	Intercept	DBH	Height
PIPO	120	0.700	0.703	1.2387	0.1439	-
PIEN	120	0.716	0.540	1.5346	0.1414	-0.0919
PIFL	29	0.868	0.622	0.1806	1.4446	_
PIPU	24	0.385	0.769	1.3823	0.0754	_
POTR	112	0.493	0.501	1.2797	0.1521	-
PSME	62	0.595	1.237	1.8310	0.0945	_

Appendix 3. Comparison of kriging models

We calculated root mean square error (RMSE), mean absolute error (MAE), and R^2 values for each kriging model: one including both canopy cover and heat load index (HLI), one with only canopy cover, one with only HLI, and one with no covariates. The model using both HLI and canopy cover had the highest R^2 and the lowest MAE values. We extracted canopy cover for each 4 \times 4 m grid cell in the spatiotemporal interpolation grid from the allometrically-derived crown diameters for each tree at the site using the st_intersection function in the sf package in R (Pebesma and Bivand 2005; Pebesma and Bivand 2023).

Covariate included	R ²	MAE	RMSE
cover + hli	0.38	12.12	22.86
cover	0.36	12.28	23.09
hli	0.38	12.18	22.85
No covariate	0.37	12.30	22.92